Journal of Materials Research and Technology 27 (2023) 7627–7635

Contents lists available at ScienceDirect

Journal of Materials Research and Technology

journal homepage: www.elsevier.com/locate/jmrt

Flattening aluminum plates with tuning asymmetric rolling parameters

Hui Su [a], Longgang Hou [b,c,*], Qingkun Tian [a], Yawen Wang [a], Linzhong Zhuang [d,e,**]

[a] State Key Laboratory for Advanced Metals and Materials, University of Science and Technology Beijing, Beijing, 10083, China
[b] BCAST, Brunel University London, Kingston Lane, Uxbridge, Middlesex, UB8 3PH, United Kingdom
[c] Nanjing Institute for Advanced Transportation Equipment and Technology, No.8 Lanhua Road, Pukou District, Nanjing, 211800, China
[d] Beijing Advanced Innovation Center for Materials Genome Engineering, University of Science and Technology Beijing, Beijing, 10083, China
[e] Beijing Laboratory of Metallic Materials and Processing for Modern Transportation, University of Science and Technology Beijing, Beijing, 10083, China

ARTICLE INFO

Handling editor. L Murr

Keywords:
Aluminum alloy plate
Asymmetric rolling
Bending
Deformation

ABSTRACT

The asymmetric rolling (ASR) process can introduce shear strains inside the plate, resulting in the improvements of microstructures and mechanical properties. Its industrial application for rolling the (mid-)thick plates is impeded by the uncontrollable bending behavior. In this study, the influences of rolling parameters on the bending behavior of the rolled AA 7050 aluminum alloy plates were investigated. It is found that the plate will bend towards the slower roll with larger speed ratios and initial plate thickness as well as lower thickness reduction. A flat plate can be obtained by choosing appropriate rolling parameters. The equivalent plastic strain rate distribution is considered to be critical to the plate bending, the downward bending (towards faster roll) would be associated with an obvious increase of the equivalent plastic strain rate at the top surface of the plate near the end of the deformation zone. Multi-pass asymmetric rolling routes considering bending optimization were proposed and verified through rolling trials. As the speed ratio increased from 1.1 to 1.2, the through-thickness plastic strain became more homogeneous and the total rolling pass numbers decreased by 33 % (from 9 passes to 6 passes).

1. Introduction

High-strength aluminum alloys plates manufactured by traditional multi-pass symmetric hot rolling (SR) are widely used as lightweight structural materials in modern transportation and aircraft industries [1,2], The which usually exhibit inhomogeneous through-thickness plastic deformation, microstructures and mechanical properties [3–5]. The main reason is that the shear strains are mainly concentrated near the plate surface due to severe friction between the workpieces and the working rolls [6,7]. The asymmetric rolling (ASR) process with smaller rolling forces and torques [8,9] can introduce shear strains into the plate center effectively, improving the plastic strain homogeneity as well as the total strain level, contributing to microstructure refinement and better mechanical properties [10–12]. The ASR process can be achieved through different rotational speeds, working roll diameters, friction conditions, temperature gradients, or a combination of these parameters. It is considered to be suitable for producing (mid-)thick plates with some undissolved issues.

It is known that the ASR process is often accompanied with bending problem, which hinders its industrial application [13]. Although the bending can be easily eliminated when rolling thin sheets, it is difficult to be overcome during multi-pass hot rolling of the (mid-)thick plates [14,15]. For example, the upward bending may prevent the plate biting into the roll gap in the next pass [14], while the downward bending may damage the roll table [15]. The influences of the rolling parameters on the plate bending are widely investigated. Among all rolling parameters, the speed ratios can greatly affect the bending, i.e., the workpieces are usually bent towards the slower roll [16–18]. The thickness reduction can also influence the plate bending. It was found that the ASR-ed plate will be bent towards slower roll at small thickness reduction but toward faster roll at larger thickness reduction [13,19]. Ma et al. [20] found that the required thickness reduction to prevent plate bending during the ASR process was smaller at the later passes (i.e., a smaller initial thickness), which means the thicker plates may be more likely to bend towards the slower roll. Other factors such as temperature [21] and friction [22] can also affect the plate bending behavior.

* Corresponding author. Nanjing Institute for Advanced Transportation Equipment and Technology, No.8 Lanhua Road, Pukou District, Nanjing, 211800, China.
** Corresponding author. Beijing Advanced Innovation Center for Materials Genome Engineering, University of Science and Technology Beijing, Beijing 10083, China.
E-mail addresses: lghou@live.com (L. Hou), linzhongzhuang@163.com (L. Zhuang).

https://doi.org/10.1016/j.jmrt.2023.11.204
Received 8 October 2023; Received in revised form 13 November 2023; Accepted 22 November 2023
Available online 25 November 2023

Table 1
List of abbreviations.

Abbreviation	Definition
i	Speed ratio
h_0	Initial plate thickness
Δh	Thickness reduction
Δh_{crit}	Critical thickness reduction
h	Thickness after rolling
D	Roll diameter
R	Curvature radius
K	Curvature index
v_u	Materials flow speed at the top surface
v_l	Materials flow speed at the bottom surface
ω	Angular velocity
HSRB	High strain rate band

Table 2
Rolling parameters for rolling simulation.

Parameter	Symbol	Value/Range
Rolling temperature (°C)	T	400
Friction coefficient	μ	0.35
Speed ratio	i	1–2
Initial plate thickness (mm)	h_0	10–40
Thickness reduction (%)	Δh	10–51
Roll diameter (mm)	D	400

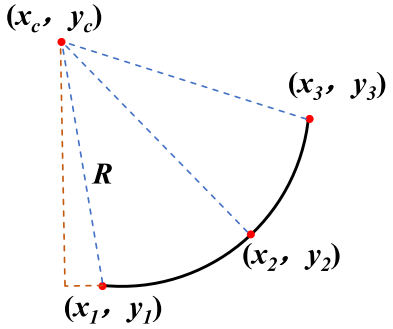

Fig. 1. Illustration for the calculation of curvature radius.

Many efforts have been concentrated on the causes of the bending phenomenon. The theoretical analysis considered that the strains (or strain rates) might be the main reason for bending, although there is still controversy over how it works. Salimi et al. [23] and Qwamizadeh et al. [24,25] explained the plate bending through the slab method: The axial strains and shear strains were accumulated in the deformation zone during the asymmetric rolling, and the bending direction and the curvature radius could be obtained by calculating their effects separately. In other side, Cho et al. [26] simulated the asymmetric rolling of AZ31B alloy and considered that the shear strain rate differences between the top and bottom layers at the biting region could cause the variation of plate bending. Kasai et al. [27] found that the bending was closely related to the shear band distribution. Our previous work compared the distribution of shear bands under different speed ratios and thickness reductions, and found that the plate would bend downward if the shear bands reached the top surface at the end of the deformation zone [28].

The plate bending can be influenced by different rolling parameters simultaneously. However, previous studies were mostly focusing on the impacts of single parameter on the plate bending behavior, and few studies considered the bending control by adjusting different rolling parameters at the same time. The continuous multi-pass asymmetric rolling process can be widely applied for the (mid-)thick plates if the bending problem could be solved along with mechanistic understanding. This study simulated the effects of the ASR parameters on the plate bending behavior at first and then analyzed the bending behavior by the equivalent strain rate and node acceleration. Finally, the multi-pass ASR processes with bending optimization were proposed and verified. Abbreviations in this study are listed in Table 1.

2. Method and experiments

Finite element analysis for hot rolling was conducted with the software MSC. Marc. A 2-D model with plane strain state was established to reduce the calculating time as the plate widespread during asymmetric rolling was ignored. The material data [29] of AA7050 aluminum alloy and coulomb friction condition (friction coefficient $\mu = 0.35$) were used. The plate was set as a deformable part with a rectangular element size of 1 mm. The working roll, roll table and pusher were assumed to be rigid bodies. The rotation speed of the upper roll was constant while the lower roll was rotated at different speeds. The rolling parameters were listed in Table 2.

The rolling experiments were conducted using the asymmetric rolling mill. The working rolls are driven separately by two electrical motors to obtain speed mismatch. Before rolling, the homogenized AA 7050 aluminum alloy plates with 20 mm initial thickness were held in an air furnace for 40 min to achieve uniform temperature. Grid lines were carved on the side of the plate (RD-ND plane) for comparison between the simulations and experiments.

As illustrated in Fig. 1, three points were randomly collected at the top (or bottom) surface of the rolled plate, the curvature radius (R) and curvature index (K) were calculated as follows [30,31]:

$$\begin{cases} (x_1 - x_c)^2 + (y_1 - y_c)^2 = R^2 \\ (x_2 - x_c)^2 + (y_2 - y_c)^2 = R^2 \\ (x_3 - x_c)^2 + (y_3 - y_c)^2 = R^2 \\ |K| = 1/R \end{cases} \quad (1)$$

where (x_1, y_1), (x_2, y_2), (x_3, y_3) were the coordinates of the selected points and (x_c, y_c) was the assumed curvature center coordinate. $|K|$ is the reciprocal of the curvature radius R and a smaller $|K|$ value corresponds to a flatter plate. The positive K value reflects upward bending and vice versa.

3. Results and discussion

3.1. Validating of the rolling simulation

Fig. 2 shows good agreement between the FE simulations and rolling experiments and the simulations should be reliable. The plate may bend upward or downward under different rolling conditions (Fig. 2a and b). It is worth noting that the plate bending can be suppressed under certain rolling conditions (Fig. 2c and d). The inclination angles of the grid lines after rolling are consistent with the simulation results with an average error <5 % (Fig. 2e and f).

3.2. Curvature evolution during the ASR process

It is widely believed that the ASR-ed plates are more likely to bend towards the slower roll with the increase of the speed ratio [14,26]. Fig. 3 shows the influences of the speed ratio on the plate bending with 10–50 % thickness reduction. For small thickness reductions (i.e., $\Delta h =$ 10 %), the plates are always bent upward and stuck to the upper roll ($K = 5$) for all speed ratios. For medium thickness reductions (i.e., $\Delta h = 20$ % and 30 %), the curvature index K increased gradually from negative to positive with speed ratios and becomes almost zero at the speed ratio of ~1.15 ($\Delta h = 20$ %) and ~1.3 ($\Delta h = 30$ %), which means the bending direction is changed. Further increasing the speed ratio shows no significant impact on plate bending. For larger thickness reductions (i.e., $\Delta h = 40$ % and 50 %), the downward bending trend (toward the faster roll) becomes unavoidable no matter how the speed ratio increases. This indicates that the thickness reduction is a key factor to affect the plate

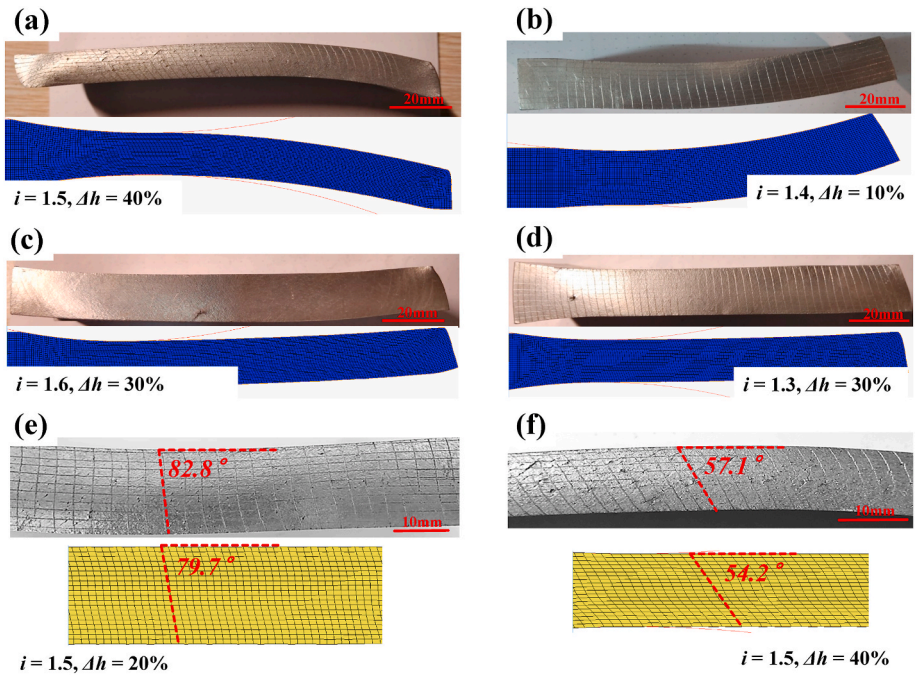

Fig. 2. Experimental and simulation results about (a–d) the plate bending and (e, f) the inclination of the grid lines.

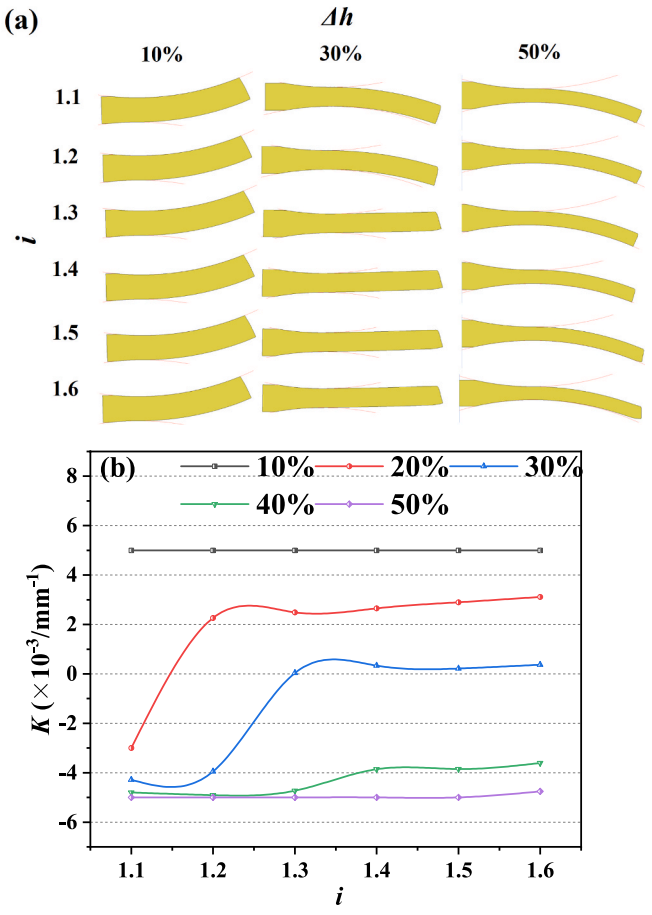

Fig. 3. Plate bending under different speed ratios: (a) simulation results; (b) influences of the speed ratio on the curvature index *K*.

bending.

Fig. 4a shows the influences of thickness reduction on the plate bending under different speed ratios. The *K* value is decreased from positive to negative as the thickness reduction increases for all speed ratios, referring to an intensified downward bending trend. The "critical thickness reduction" (Δh_{crit}) that can prevent the plate bending ($K = 0$) increased to ~43 % first and remained almost unchanged with speed ratios (Fig. 4b). This indicates that the downward bending trend cannot be eliminated by increasing the speed ratio once the applied thickness reduction exceeds the maximum Δh_{crit}. If the applied Δh is smaller than the maximum Δh_{crit}, the downward bending can be suppressed by increasing speed ratio.

During the multi-pass symmetric/asymmetric rolling, the plate thickness will be decreased gradually after each pass and the influence of the inlet plate thicknesses (same to initial plate thickness) on the plate bending needs to be cleared. Fig. 5 shows the evolution of the curvature index *K* with initial thickness. For small speed ratios, i.e., $i = 1.1$, the downward bending is more evident than other conditions. The plates with $h_0 < 20$ mm are even attached to the lower roll ($K = -5 \times 10^{-3}$) after rolling. The downward bending could be suppressed for the plates with $h_0 = 38$ mm and 40 mm. Increasing the speed ratio to 1.2, the upward bending trend is intensified and the required h_0 for flat plate is reduced to ~30 mm. For the speed ratios $i > 1.3$, the bending curvature index *K* are almost equal and the bending can be suppressed for $h_0 = 20$ mm. An upward bending trend can be observed with larger initial thickness.

3.3. Bending optimization and multi-pass rolling trials

It can be seen from the above results that the plate bending behavior can be simultaneously influenced by all rolling parameters. A flat plate can be obtained through an appropriate ASR parameter combination. The critical thickness reductions (Δh_{crit}) for different initial plate thicknesses and speed ratios are shown in Fig. 6a. The Δh_{crit} increases with speed ratios first (the left side of the dotted line in Fig. 6a, which varies with the initial plate thickness) and remains constant thereafter (the right side of the dotted line in Fig. 6a). The plate will be bent downward if the applied plate thickness is larger than Δh_{crit}, or else, it will be bent upward. Two additional situations were measured near the maximum

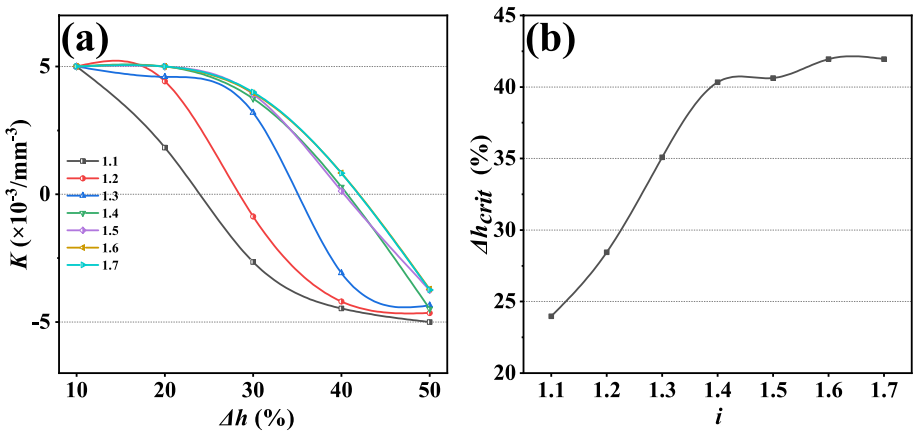

Fig. 4. Plate bending under different thickness reductions: (a) influences of thickness reductions on curvature index *K*; (b) critical thickness reduction for flat plate. (

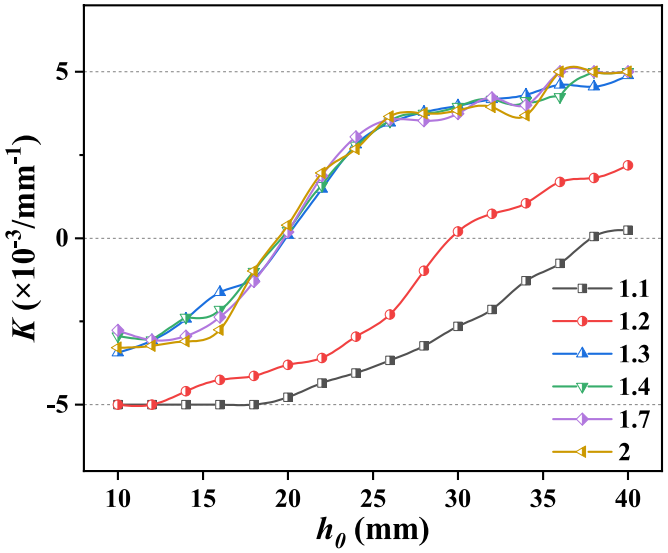

Fig. 5. Curvature index K under different initial thickness. (initial plate thickness h_0 = 10–40 mm, speed ratio i = 1.1–2 and thickness reduction Δh = 30 %).

Δh_{crit} value (as illustrate in Fig. 6c, the applied Δh for point 1 and 2 are 3 % larger or smaller than Δh_{crit}, respectively) to explore the causes for the plate bending and will be discussed in the next section. The rolled plate thickness under each rolling condition is calculated as shown in Fig. 6b. Several parameter combinations can be used to obtain flat plates with same final plate thickness (the points where the curves intersect with the dotted line in Fig. 6b). For example, a flat 20 mm plate can be obtained by single-pass asymmetric rolling with h_0 = 28 mm and i = 1.2, or h_0 = 32 mm and i = 1.3, or h_0 = 36 mm and i = 1.4. Two multi-pass asymmetric rolling routes with bending optimization are proposed as given in Table 3. The ASR parameters are as follows: D = 450 mm, h_0 = 20 mm, total thickness reduction Δh = 70 % with speed ratios i = 1.0, 1.1, and 1.2. For each rolling pass, the required Δh_{crit} for i = 1.2 is higher than that for i = 1.1, and the required passes to achieve same total reduction Δh = 70 % are reduced from 9 to 6 passes.

Fig. 7a shows the plates without severe bending can be obtained through these two routes. Fig. 7b and c shows the plates exhibit good bending resistance after the 2nd and 4th pass (i = 1.1). To clarify whether the simulated parameter combination is necessary for bending control, two additional rolling processes with i increased from 1.1 to 1.2 only at the 4th and 6th pass were conducted and severe upward bending can be observed (Fig. 7d and e), indicating the importance and feasibility of bending control with ASR parameter optimization.

Fig. 8 shows the through-thickness equivalent plastic strain distributions after the SR and ASR processing. The equivalent plastic strain accumulated at the plate center increased with speed ratio, resulting in more homogeneous deformation along with diminished equivalent plastic strain difference between the surface and plate center (from 0.86 (i = 1) to 0.63 (i = 1.2)) (Fig. 8a and b). For the SR processing, the shear strains are mainly concentrated near the surface layers. For the ASR process, the shear strains at the plate center are increased from 0.18 (i = 1.1) to 0.34 (i = 1.2). The grid lines in Fig. 8c–e are changed from "C"-shape to "S"-shape, inclined and stretched along rolling direction as the speed ratio increases, indicating higher shear strain accumulation inside the plate [32,33].

3.4. Reasons for plate bending

The plate bending is related to the through-thickness material flow speed gradient (as illustrated in Fig. 8a). Taking upward bending as an example, the flow speed at the top and bottom surfaces can be expressed as follows,

$$\begin{cases} v_u = \omega R \\ v_l = \omega(R+h) \\ v_l/v_u = 1+h/R \end{cases} \quad (2)$$

where v_u and v_l are material flow speeds at the top and bottom surface, R and h are the curvature radius and finial plate thickness, ω is the angular velocity. With the increase of the curvature radius R, the flow speed gradient decreases. Lu et al. [34] calculated the material flow speed at the top and bottom surfaces and found that the plate will leave the rolling gap without any curvature under equal material flow speeds. Fig. 9b–d shows the changes of the flow speeds at the top and bottom surfaces during asymmetric rolling, which indicates that the flow speeds at the top surface are increased twice at the roll-biting and outgoing regions and are kept equal to the linear velocity of the upper roll in the middle region. With the increase of speed ratio (comparing Fig. 9b and d), the material flow at the bottom surface is accelerated and faster than that at the top surface and the bending direction is changed. With the increase of the thickness reduction (comparing Fig. 9c and d), the increase of material flow speed at the top surface is more significant than that at the bottom surface. The flow speed gradient between two surfaces is reduced, resulting in a flatter plate.

The increase of the flow speed, i.e., acceleration, especially for the top surface near the end of the deformation zone, plays a critical role in the plate bending. The direction and magnitude of the acceleration vector can be used to describe the plate bending: the outgoing part of the plate can be considered to move in a uniform circular motion around the center and there is a centripetal acceleration towards the center of the

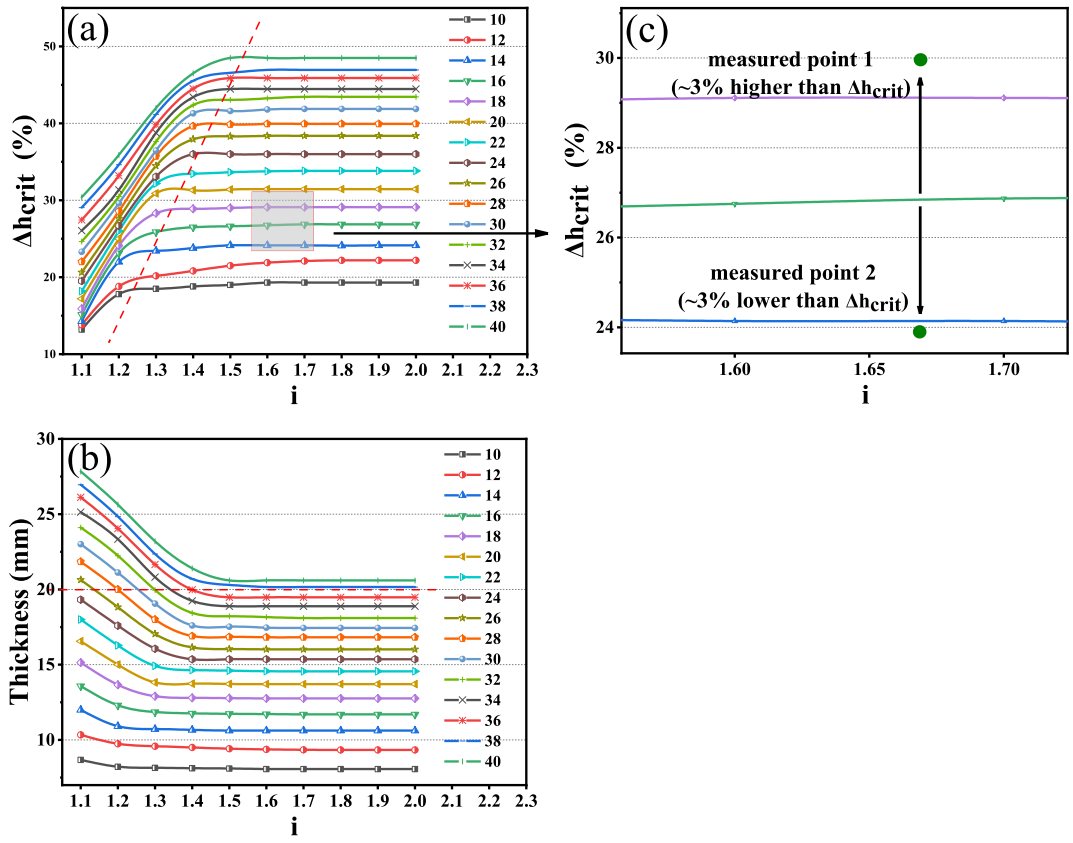

Fig. 6. Rolling conditions with bending optimization: (a) required critical thickness reduction under different speed ratios and initial thicknesses, (b) final thickness of flat plates under different rolling conditions, (c) enlarged image of (a).

Table 3
Rolling schedule for two multi-pass asymmetric rolling routes.

Pass number	Thickness after each pass/mm	
	1.1	1.2
0	20	20
1	16.7 (16.5 %)	15.2 (24 %)
2	14.2 (14.9 %)	11.9 (21.7 %)
3	12.2 (14.1 %)	9.4 (21 %)
4	10.5 (13.9 %)	8 (14.9 %)
5	9.1 (13.3 %)	6.9 (13.8 %)
6	7.9 (13.2 %)	6 (13 %)
7	7.1 (10.1 %)	–
8	6.5 (8.5 %)	–
9	6 (7.7 %)	–

circle. The plate bending is closely related to the plastic strain or strain rate [35,36]. Kasai et al. [27] found that the materials acceleration could be related to the plastic strain rate and the equivalent plastic strain rate distribution is used for bending analysis. Fig. 10 shows the distribution of the acceleration vector under different bending conditions. After the workpiece is bitten into the roll gap, two accelerations are generated at the surface layers individually and transmitted into the plate center as the rolling process continues. The acceleration transmission direction will change after their interaction inside the plate or interacted by the top/bottom roll, resulting in different distribution. Previous work [28] has explained the interaction mechanism among the accelerations (or with the working rolls). If the acceleration vector is transmitted downwards and reaches the bottom surface near the end of the deformation zone (Fig. 10a), an upward bending will occur due to the suppression of the lower roll, or else, the plate will bend downward (Fig. 10c). There is a balance state that can keep the plate straight (Fig. 10b).

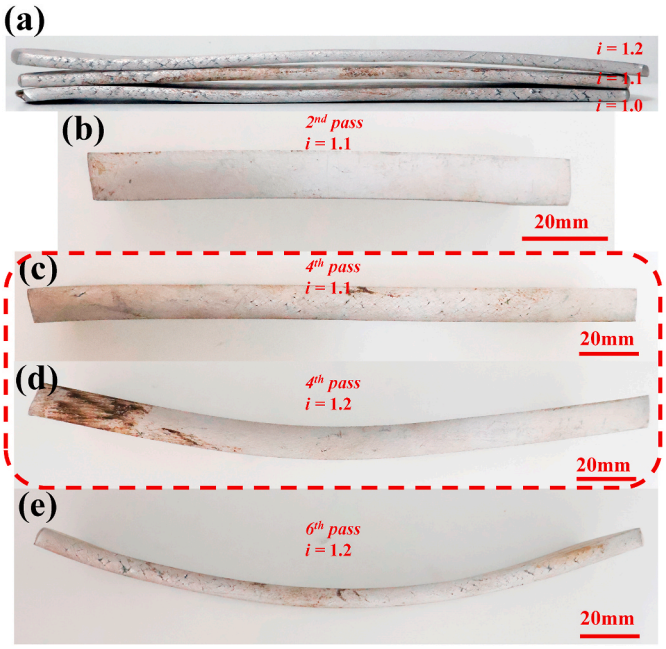

Fig. 7. Shape of the rolled plate: (a) after rolling with $i = 1.0$, 1.1 and 1.2, (b) after 2nd pass with $i = 1.1$, (c) after 4th pass with $i = 1.1$, (d) $i = 1.2$ at the 4th pass and (e) $i = 1.2$ at the 6th pass. The thickness reduction per pass of the symmetric rolling ($i = 1.0$) is the same as that of $i = 1.1$.

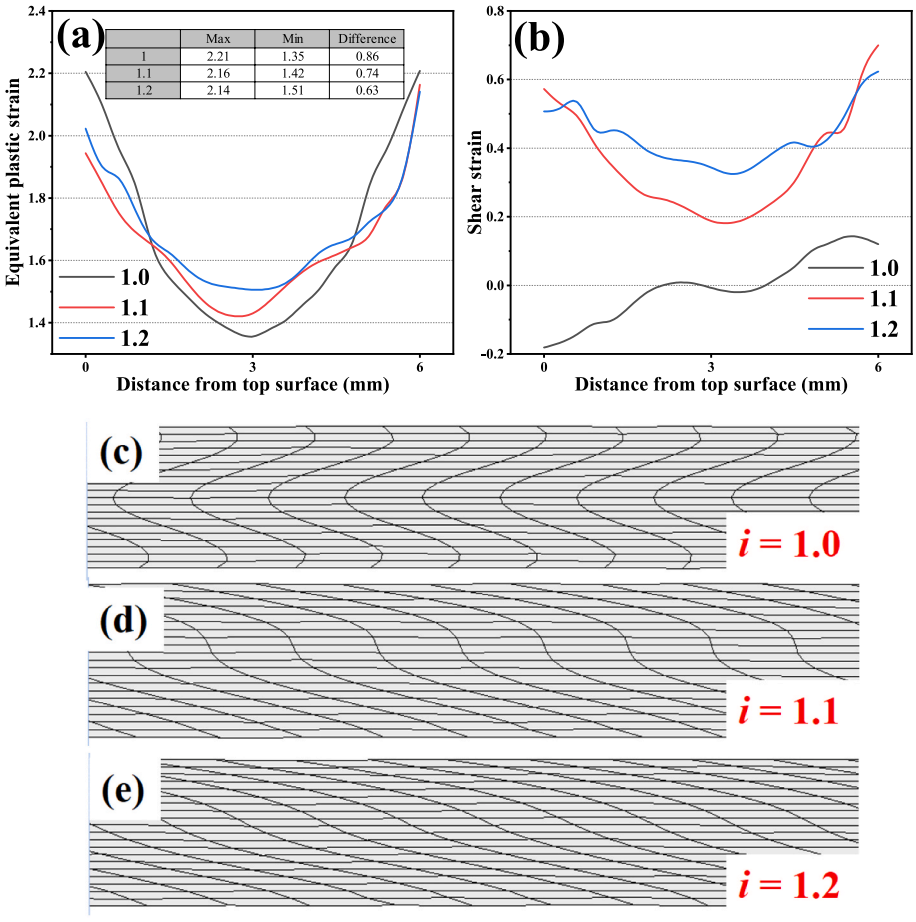

Fig. 8. Through-thickness strain distribution: (a) equivalent plastic strain, (b) shear strain, and (c–e) deformed grid lines with different speed ratios.

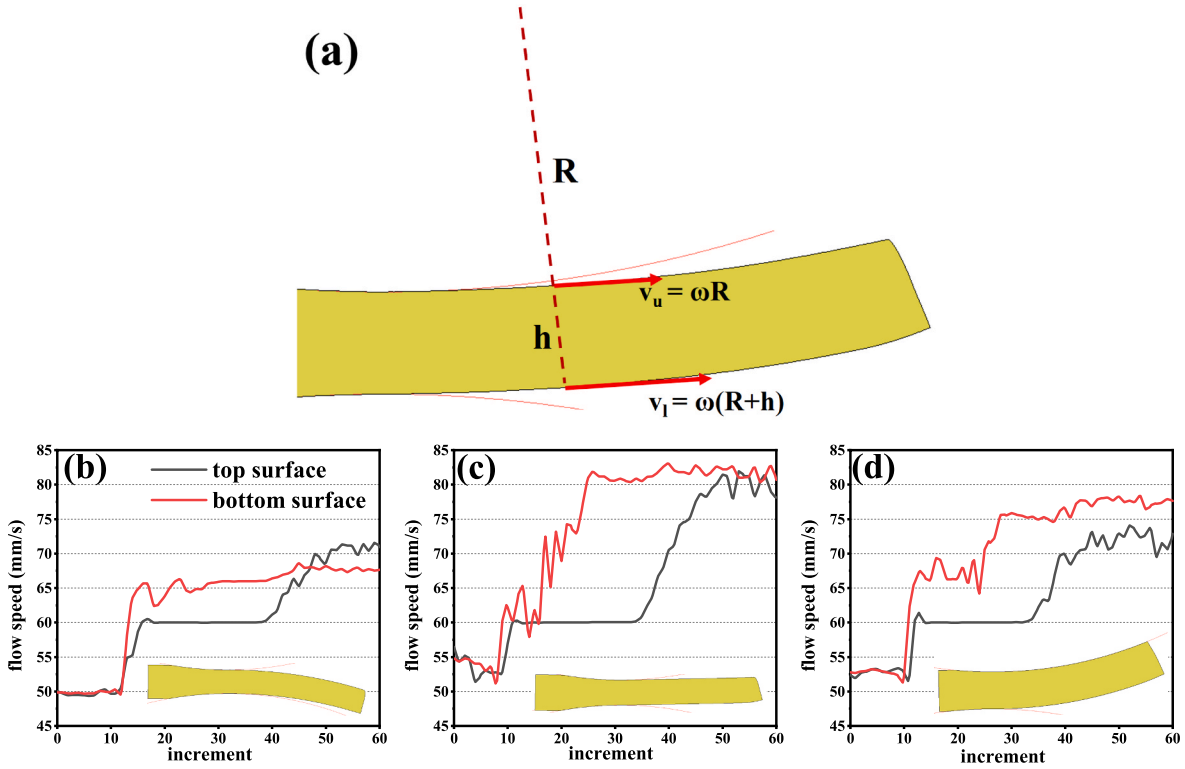

Fig. 9. Flow speeds at the top and bottom surfaces: (a) illustration of the speed gradient, (b) downward bending ($h_0 = 30$ mm, $i = 1.1$, $\Delta h = 30$ %), (c) flat plate ($h_0 = 30$ mm, $i = 1.5$, $\Delta h = 40$ %), (d) upward bending ($h_0 = 30$ mm, $i = 1.5$, $\Delta h = 30$ %).

3.5. Analysis of downward bending

As mentioned before, the plate may bend towards the faster roll with smaller speed ratio or larger thickness reduction. If the applied Δh is smaller than the maximum Δh_{crit}, the downward bending can be effectively suppressed by increasing the speed ratios, and conversely the plate will bend downwards no matter how the speed ratio is increased when the applied Δh is higher than the maximum Δh_{crit}. Although the downward bending is caused by the acceleration (or plastic strain rate) concentration at the top surface near the end of the deformation zone, there may be differences between these two situations.

Fig. 11 shows the equivalent plastic strain and acceleration distribution for the first case. The red-dotted lines in Fig. 11a and c reflect the end of the deformation zone. For a small speed ratio, the band-like region with high equivalent plastic strain rate (named as high strain rate band, HSRB) generated at the bottom surface is more inclined and can reach the top surface closing to the end of the deformation zone. According to the acceleration vector in Fig. 11b and d, one can find that the HSRB generated at the top and bottom surfaces near the roll biting region are transmitted inside the plate till their interaction, and then the weaker HSRB from the top surface changes its direction while the stronger one from the bottom surface still keeps its direction along with slight inclination (~15°). With the increase of speed ratios, the influence of the upper HSRB to the lower HSRB is weakened. The HSRB from the bottom surface maintains its transmission direction and reaches the top surface earlier and then changes its transmission direction downwards due to the compression of the upper roll and reaches the bottom surface again at the end of the deformation zone, causing upward plate bending due to the suppress of the lower roll.

For the second case, as reported by Kasai et al. [27] and Pawelski [37], the HSRB distribution is much more complex with larger thickness reduction. The HSRB distribution under different rolling conditions will turn from a "Y"-shaped distribution (as illustrated in Fig. 11) to an "X + Y"-shaped distribution (high Δh and small i) or "intensified Y″-shaped distribution (high Δh and i) [28]. In both cases, a new through-thickness HSRB will be generated from the bottom surface and arrive at the top surface at the end of the deformation zone, resulting in downward plate bending due to the suppress of the upper roll regardless of the speed ratios.

Additional simulations are conducted (with speed ratio $i = 2.0$): the thickness reduction about 3 % higher or lower than the maximum Δh_{crit} (as illustrated in Fig. 6c) are selected for different h_0. The equivalent plastic strain rate distributions are shown in Fig. 12. For Δh lower than the maximum Δh_{crit}, the "Y"-shaped HSRB distributions with only one through-thickness HSRB are generated from the bottom surface for all conditions, which arrives at the top surface around the middle of the deformation zone, leading to an upward plate bending. For the Δh higher than the maximum Δh_{crit}, the "intensified Y″-shaped HSRB distributions with a second through-thickness HSRB generated from the bottom are observed for all conditions. This additional through-thickness HSRB reaches the top surface near the end of the deformation zone, resulting in an unavoidable downward plate bending.

4. Conclusions

This study aims at the mechanistic understanding about the bending behavior during the asymmetric rolling of high-strength aluminum alloy plates, especially the influences of rolling parameters on the bending behavior. Multi-pass asymmetric rolling processes with bending optimization are proposed via FE simulations and verified through experiments. The main findings in this study are as follows:

1. It shows that the ASR parameters can affect the plate bending behavior and the plate is more likely to bend towards the slower roll with a higher speed ratios, larger initial thickness, and smaller thickness reduction.
2. A flat plate can be obtained by selecting appropriate rolling parameters. The critical thickness reduction for bending control increases

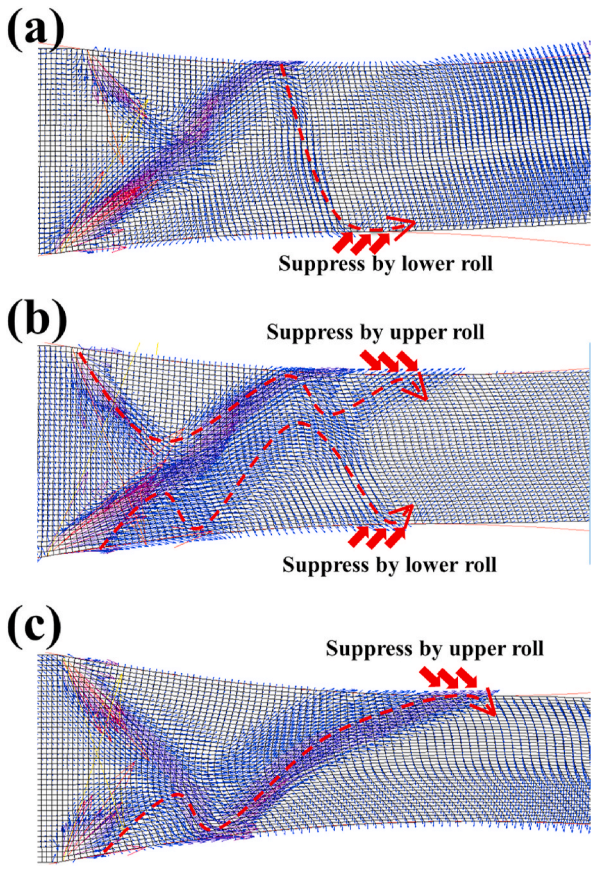

Fig. 10. The distribution of acceleration vector under different rolling conditions: (a) upward bending: $h_0 = 20$ mm, $i = 1.3$, $\Delta h = 20$ %, $D = 400$ mm, (b) flat plate (no bending): $h_0 = 20$ mm, $i = 1.3$, $\Delta h = 30$ %, $D = 400$ mm, (c) downward bending: $h_0 = 20$ mm, $i = 1.3$ $\Delta h = 40$ %, $D = 400$ mm.

first and remains constant as the speed ratio increases. Once the applied thickness reduction exceeds the maximum value of the critical thickness reduction, the plates will bend toward the faster roll.

3. The plate bending behavior during the asymmetric rolling can be related to the equivalent plastic strain rate distribution. The plate bends downwards when a high strain rate band reaches the top surface at the end of the deformation zone.
4. Multi-pass asymmetric rolling routes are successfully applied to flatten the plates. Increasing the speed ratios can help to reduce the pass numbers and improve the through-thickness strain homogeneity by introducing more shear strains inside the plates.

Different multi-pass asymmetric rolling routes for flattening the plates may cause different influences on the plastic strain distributions, microstructures and mechanical properties, which will be the future focus.

Credit author statement

Hui Su: Conceptualization, Data curation, Formal analysis, Methodology, Investigation, Writing - Original draft. **Longgang Hou:** Conceptualization, Supervision, Writing - Review & Editing, Visualization, Funding acquisition. **Qingkun Tian:** Investigation, Data curation. **Yawen Wang:** Investigation, Data curation, Validation. **Linzhong Zhuang:** Supervision, Writing - Review & Editing, Funding acquisition.

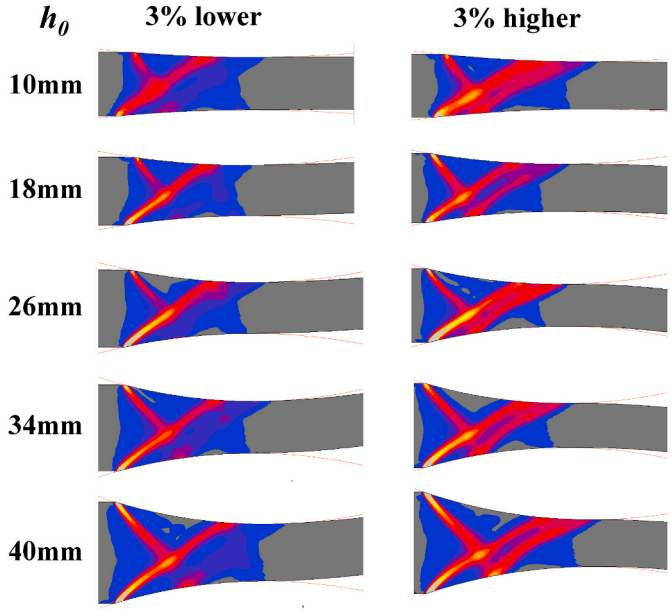

Fig. 12. Equivalent plastic strain rate distributions for different h_0 and Δh (3 % smaller or larger than the maximum Δh_{crit}).

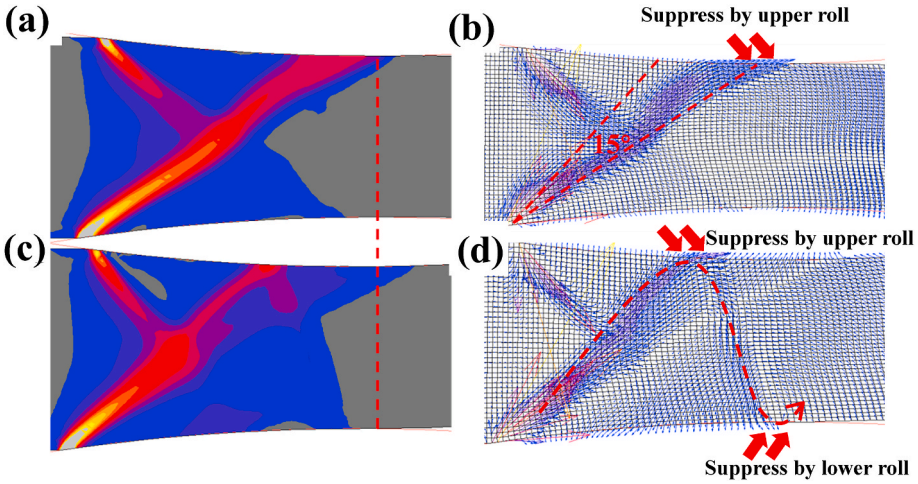

Fig. 11. Equivalent plastic strain rate and acceleration distribution under different rolling conditions: (a, b) downward bending: $h_0 = 20$ mm, $i = 1.1$, $\Delta h = 20$ %, (c, d) upward bending: $h_0 = 20$ mm, $i = 1.3$, $\Delta h = 20$ %.

Declaration of competing interest

The authors declare that they have no known competing financial interests or personal relationships that could have appeared to influence the work reported in this paper.

Acknowledgement

The authors are grateful for the financial supports from the Constructed Project for Key Laboratory of Beijing, China [No. BJSJ2019004], and the State Key Laboratory for Advanced Metals and Materials of China [No. 2018Z-23]. L. H. and L. Z. also acknowledge the supports from CHINALCO.

References

[1] Kazemi-Navaee A, Jamaati R, Aval HJ. Asymmetric cold rolling of AA7075 alloy: the evolution of microstructure, crystallographic texture, and mechanical properties. Mater Sci Eng 2021;824:141801.
[2] Guo Y, Zhang M, Wang Z, Wang S, Liu C, Qian L, et al. Effects of cold temperatures, strain rates and anisotropy on the mechanical behavior and fracture morphology of an Al-Zn-Mg-Cu alloy. Mater Sci Eng 2021;806:140691.
[3] Li X, Li X, Ye Y, Zhang R, Kure-Chu SZ, Tang G. Deformation mechanisms and recrystallization behavior of Mg-3Al-1Zn and Mg-1Gd alloys deformed by electroplastic-asymmetric rolling. Mater Sci Eng 2019;742:722–33.
[4] Taali S, Moazzen P, Toroghinejad MR, Chen G, Mola J. Microstructure, texture, and mechanical properties of asymmetrically cold-rolled Ni1.5FeCrCu0.5 high-entropy alloy. J Mater Res Technol 2022;21:3489–501.
[5] Wu W, Chen X, Pan F. Effect of Y content on the microstructure and mechanical anisotropy of Mg-6Zn-xY-0.5Ce-0.4Zr alloy subjected to asymmetric rolling. Mater Sci Eng 2023;882:145465.
[6] Zuo YB, Fu X, Cui JZ, Tang XY, Mao L, Li L, et al. Shear deformation and plate shape control of hot-rolled aluminium alloy thick plate prepared by asymmetric rolling process. Trans Nonferrous Metals Soc China 2015;24(7):2220–5.
[7] Ma C, Hou L, Zhang J, Zhuang L. Effect of deformation routes on the microstructures and mechanical properties of the asymmetrical rolled 7050 Aluminum alloy plates. Mater Sci Eng 2018;733:307–15.
[8] Jeong HT, Kim WJ. Effect of roll speed ration on the texture and microstructural evolution of an FCC high-entropy alloy during differential speed rolling. J Mater Sci Technol 2022;111:153–66.
[9] Xie Y, Deng Y, Wang Y, Guo X. Effect of asymmetric rolling and subsequent ageing on the microstructure, texture and mechanical properties of the Al-Cu-Li alloy. J Alloys Compd 2020;836:155445.
[10] Ko YG, Kim YG, Hamad K. Microstructure optimization of low-carbon steel using differential speed rolling deformation followed by annealing. Mater Lett 2020;261:127154.
[11] Tamimi S, Gracio JJ, Lopes AB, Ahzi S, Barlat F. Asymmetric rolling of interstitial free steel sheets: microstructural evolution and mechanical properties. J Manuf Process 2018;31:583–92.
[12] Razani NA, Dariani BM, Soltanpour M. Microstructure and mechanical property improvement of X70 in asymmetrical thermomechanical rolling. Int J Adv Des Manuf Technol 2018;97:3981–97.
[13] Hao L, Di HS, Gong DY. Analysis of sheet curvature in asymmetrical cold rolling. J Iron Steel Res Int 2013;20(5):34–7.
[14] Anders D, Münker T, Artel J, Weinberg K. A dimensional analysis of front-end bending in plate rolling applications. J Mater Process Technol 2012;212:1387–98.
[15] Son RC, Sim KH, Sh O. FE simulation of the influence of roll diameter difference on the plate curvature during hot plate rolling. Steel Res Int 2018;90(4):1800007.
[16] Farhat-Nia F, Salimi M, Movahhedy MR. Elasto-plastic finite element simulation of asymmetrical plate rolling using an ALE approach. J Mater Process Technol 2006;177:525–9.
[17] Kraner J, Fajfar P, Palkowski H, Kugler G, Godec M, Paulin I. Microstructure and texture evolution with relation to mechanical properties of compared symmetrically and asymmetrically cold rolled aluminum alloy. Metals 2020;10(2):156.
[18] Hao P, Liu J. Influence of snake rolling on metal flow in hot rolling of aluminum alloy thick plate. Mech Ind 2020;21(5):525.
[19] Wang W, Lu S. Finite element analysis of the deformation behavior of the up and down roll differential diameter rolling for medium plate. J Phys Conf 2020;1653(1):012054.
[20] Ma C, Hou L, Zhang J, Zhuang L. Microstructures and properties of asymmetrical rolled 7050 Al alloy plate with bending behavior optimization. Mater Sci Eng 2016;657:322–30.
[21] Zhang T, Wu Y, Gong H, Shi W, Jiang F, Jiang S. Analysis of temperature asymmetry of aluminum alloy thick plate during snake hot rolling. Int J Adv Manuf Technol 2016;87:941–8.
[22] Knight CW, Hardy SJ, Lees AW, Brown KJ. Investigations into the influence of asymmetric factors and rolling parameters on strip curvature during hot rolling. J Mater Process Technol 2003;134:180–9.
[23] Salimi M, Sassani F. Modified slab analysis of asymmetrical plate rolling. Int J Mech Sci 2002;44:1999–2023.
[24] Qwamizadeh M, Kadkhodaei M, Salimi M. Asymmetrical sheet rolling analysis and evaluation of developed curvature. Int J Adv Manuf Technol 2012;61(1–4):227–35.
[25] Qwamizadeh M, Kadkhodaei M, Salimi M. Asymmetrical rolling analysis of bonded two-layer sheets and evaluation of outgoing curvature. Int J Adv Manuf Technol 2014;73:521–33.
[26] Cho JH, Kim HW, Kang SB, Han TS. Bending behavior, and evolution of texture and microstructure during differential speed warm rolling of AZ31B magnesium alloys. Acta Mater 2011;59(14):5638–51.
[27] Kasai D, Komori A, Ishii A, Yamada K, Ogawa S. Strip warpage behavior and mechanism in single roll driven rolling. ISIJ Int 2016;56(10):1815–24.
[28] Su H, Hou L, Tian Q, Wang Y, Zhuang L. Understanding the bending behavior and through-thickness strain distribution during asymmetrical rolling of high-strength aluminium alloy plates. J Mater Res Technol 2023;22:1462–75.
[29] Ma C, Hou L, Zhang J, Zhuang L. Influence of thickness reduction per pass on strain, microstructures and mechanical properties of 7050 Al alloy sheet processed by asymmetric rolling. Mater Sci Eng 2016;650:454–68.
[30] Li S, Qin N, Liu J, Zhang X. Microstructure, texture and mechanical properties of AA1060 aluminum plate processed by snake rolling. Mater Des 2016;90:1010–7.
[31] Yang J, Li S, Liu J, Li X, Zhang X. Finite element analysis of bending behavior and strain heterogeneity in snake rolling of AA7050 plates using a hyperbolic sine-type constitutive law. J Mater Process Technol 2017;240:274–83.
[32] Park JJ. Finite-element analysis of severe plastic deformation in differential-speed rolling. Comput Mater Sci 2015;100:61–6.
[33] Hamad K, Park JH, Ko YG. Finite element analysis of deformation behavior in Al-2.2 wt.%Mg alloy subjected to differential speed rolling. J Mater Eng Perform 2015;24(8):2990–3001.
[34] Lu JS, Harrer OK, Schwenzfeier W, Fischer FD. Analysis of the bending of the rolling material in asymmetrical sheet rolling. Int J Mech Sci 2000;42:49–61.
[35] Kraner J, Smolar T, Volšak D, Cvahte P, Godec M, Paulin I. A review of asymmetric rolling. Mater Technol 2020;54(5):731–43.
[36] Sui FL, Wang X, Zhao J, Ma B, Li CS. Analysis on shear deformation for high manganese austenite steel during hot asymmetrical rolling process using finite element method. J Iron Steel Res Int 2015;22(11):990–5.
[37] Pawelski H. Comparison of methods for calculating the influence of asymmetry in strip and plate rolling. Steel Res 2000;71(12):490–6.